Polish J. Chem., **76**, 443–456 (2002)

Photoconductivity and Photodielectric Properties of Diethyl 2,5-Dianilinoterephthalate Films*

by S. Nešpůrek[1] and P.K. Mačkus[2]

[1]*Institute of Macromolecular Chemistry, Academy of Sciences of the Czech Republic, Heyrovský Sq. 2, 162 06 Prague 6, and Faculty of Chemistry, Technical University of Brno, Purkyňova 118, 612 00 Brno, Czech Republic; E-mail: nespurek@imc.cas.cz*
[2]*Department of Solid State Electronics, Vilnius University, Saulétekio al. 9, corp. III, 2054 Vilnius, Lithuanian Republic*

(Received July 3rd, 2001; revised manuscript November 12th, 2001)

Photoelectric and photodielectric properties of thin films of diethyl 2,5-dianilinoterephthalate were studied. Both phenomena are strongly influenced by charge carrier trapping. A weak photodielectric response (about 0.5% and 0.01% at the frequencies 10^2 and 10^4 Hz, respectively) seems to be associated with the photoformation of free and trapped charge carriers.

Key words: photoconductivity, photodielectric effect, charge carrier trapping, diethyl 2,5-dianilinoterephthalate

The potential use of organic materials for photogeneration of free charge carriers in light-sensitive devices, and low-cost photovoltaic cells [1] as well as in electrographic recording systems has stimulated interest in their electronic properties. Photoconductivity in organics has been studied for a long time, but some details of the process are not yet fully understood. Intrinsic photogeneration has been studied in some detail for anthracene [2], tetracene [3], pentacene [4], phthalocyanine [5], and other molecular materials including polymers, like polyacetylenes [6], polysilanes [7], poly(phenylenevinylenes) [8], *etc*. One of the major achievements of these studies was the demonstration of the applicability of the Onsager model [9] of the field-assisted dissociation of a pair of charges. The results show that photogeneration occurs *via* an intermediate stage of a bonded charge pair state (charge-transfer) and its subsequent thermal dissociation, which is a thermally activated and field-assisted diffusive process. The light-induced charge transfer (charge separation) within an individual molecule or on the intermolecular level can change both molecular polarizability and dipole moment. On a macroscopic level, these changes can be detected by photodielectric spectroscopy.

In many organic molecules the ratio of the dipole moment in the excited state to that in the ground state amounts up to two. Quite large changes appear in compounds having both electron-acceptor and electron-donor substituent groups in an aromatic

*Dedicated to the memory of Professor Krzysztof Pigoń.

structure, which favour an increase in the charge separation in the excited state. Polarizability of aromatic hydrocarbons in the excited state appears to increase by some 20–70% [10], that of certain tetraphenylpolyenes may increase four times. Preliminary estimates suggest that about 18% increase in relative electric permittivity might be expected if a 1% concentration of excited species is attained. This change could make it possible to construct solar energy conversion cells on the basis of the photodielectric effect [11]. However, the singlet and triplet excited states exhibit short life-times and their direct use in energy conversion devices seem to be improbable. During the last twenty years photochemistry and photophysics has been strongly developed and new types of excited species with prolonged life-times, like localized excitons, excimers, exciplexes, ion-pairs, photochromic intermediates, *etc*., have been found and their properties studied [12–14]. These species can also participate in the photodielectric effect. Thus, the old idea of the construction of solar cells based on the photodielectric effect [11] can be developed now, using new advanced molecular electronic materials.

It could be pointed out that the photodielectric effect, *i.e*. dielectric change of a photoconductive capacitor caused by illumination, was studied in the past mainly on inorganic materials, but it was usually weak, because of small changes in polarizability and dipole moment under illumination. It was usually explained on the basis of the following hypotheses: (i) Space charge effect and polarization [15]. (ii) Polarization of traps containing loosely bound charge carriers [16]. (iii) Heterogeneous dielectric with photoconductive domains [17–19]. (iv) Increase in the free-charge carrier concentration gradient on sample illumination [20,21]; in this case the sample contacts and in particular charge the carrier injection can play an important role.

In this paper the photodielectric behaviour of thin films of diethyl 2,5-dianilinoterephthalate (DTA) is presented. It is shown, that the DTA films are photoconductive and a possible photodielectric mechanism can be explained on the basis of the hypothesis (iv). The changes in the capacitance induced by light are lower than in inorganic materials [20] (*cf*. the photocapacitance change in CdTe, where $\Delta C = 50\%$ and in DTA, where $\Delta C = 1\%$) provided that charge transfer processes are not included.

EXPERIMENTAL

Material and samples. Oligoanilines as compounds with repeating phenyleneimino units are good electron donors [22]. They are photoconductive [23] and can be substituted with electron-acceptor groups (COOH, $COOC_2H_5$), thus forming intramolecular hydrogen bond of the type C=O...H–N [24]. Diethyl 2,5-dianilinoterephthalate (DTA) (Fig. 1) was prepared by oxidation of 2,5-dianilino-1,4-dihydroterephthalate with iodine [25] and purified by several crystallizations from ethanol to a constant melting point, and subsequent sublimation at 10^{-3} Pa. Its melting point, after triple crystallization, was 416 K. The absence of ion radicals during the oxidation was checked by the electron paramagnetic resonance method. Samples were prepared by melting of a DTA powder between two SnO_2-covered glasses. A typical sample thickness was from 10 to 100 μm, electrode area *ca*. 1 cm^2.

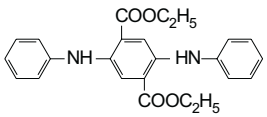

Figure 1. Diethyl 2,5-dianilinoterephthalate (DTA).

Measurements. Electrical and photoelectrical measurements were performed at pressures less than 10^{-3} Pa. The current passing through the sample was measured either directly, using a Keithley 616 electrometer, or by the compensation method, where an electrometer with a vibrating condenser was used as a zero indicator. A Keithley 240A served as the power supply. The samples were illuminated with a xenon discharge tube, monochromatized with a Zeiss SPM 1 prism monochromator. Absorption spectra were recorded with a Cary 14 spectrophotometer. Contactless measurements in an electrophotographic regime were carried out employing a rotary electrodynamic condenser electrometer [26]. Photocurrent spectra are presented as photoresponses, normalized for constant irradiance (the dependence of the photocurrent on the photon flux is not included). Dielectric and photodielectric properties were investigated using a General Radio 1621 assembly (10–10^5 Hz), which allowed to record very small capacitance changes ΔC with $\Delta C/C_0$ = 0.5 ppm accuracy (C_0 is the steady-state capacitance in the dark). The peak-to-peak amplitude of the alternating voltage was kept lower than 2 V, not to exceed the Ohmic part of the current-voltage characteristic.

RESULTS AND DISCUSSION

Photoconductivity. Optical absorption spectrum of a solid DTA film is given in Fig. 2 and summarized in Table 1. The coincidence of optical absorption bands in the solid state and of photocurrent peaks was observed for bands with the maxima at the wavelengths λ = 314 and 510 nm (*cf.* curves 1 and 2 in Fig. 2). A strong photo-

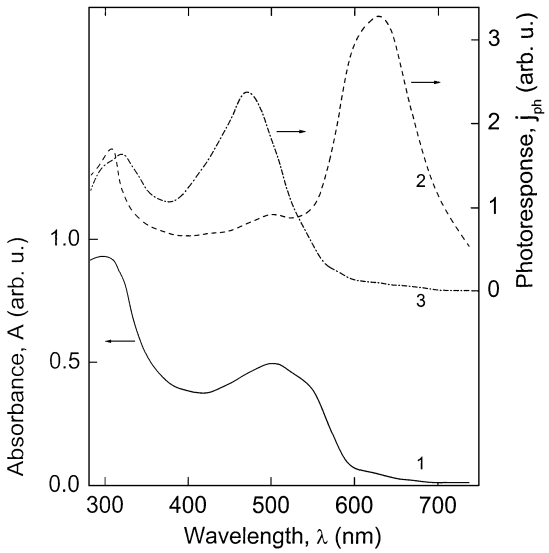

Figure 2. Absorption and photocurrent spectra of DTA. Curve 1 – absorption spectrum of sublimed layer, curve 2 – photocurrent spectrum, curve 3 – half-decay photosensitivity spectrum of DTA in poly(methyl methacrylate) matrix measured by the electrophotographic method.

conductive peak was also observed at $\lambda = 615$ nm. This band appeared during the measurements carried out both in air and *in vacuo*, if contacts were applied to the sample. A similar behaviour was also observed with *N,N′*-diphenyl-1,4-phenylenediamine [23], and it was attributed to the effect of surface precontact states and a trapped space charge at the contact interface. The situation here could be similar, because this band was not observed in contactless measurements using the xerographic method when DTA was dispersed in a poly(methyl methacrylate) matrix (*cf.* curve 3 in Fig. 2).

Table 1. Absorption maxima and photoconductivity spectral bands of DTA.

Absorption	Photoconductivity			
Solid state	Current measurement		Xerographic measurement[1)]	
λ [nm]	λ [nm]	relative intensity	λ [nm]	relative intensity
310	314	17.6	310	16.4
508	510	8.7	470	23.6
540	–	–	–	–
–	615	32.5	–	–

[1)]Contactless measurement by electrographic method (solid solution of DTA in poly(methyl methacrylate)).

The dependence of the photocurrent on the photon flux could be described by the relation $j_{ph} \approx \phi^q$, q is equal to ~ 0.5 for polychromatic light. The q coefficient slightly increased with increasing voltage applied to the sample. For the monochromatic light of wavelengths $\lambda < 520$ nm, $q = 0.3$–0.4. The activation energy of the photocurrent between 263 K < T < 294 K was $E_a^{ph} = (0.60 \pm 0.04)$ eV and voltage-independent. The activation energy of the dark Ohmic current was $E_{a1} = (0.45 \pm 0.05)$ eV ($256 < T < 294$ K) and $E_{a2} = (0.98 \pm 0.05)$ eV ($T > 294$ K). Photocurrent kinetic curve is given in Fig. 3a. The decay part consists of initial rapid drop, associated with the free carrier recombination and a slow part associated with trapping phenomena. From the decay curves, measured at different temperatures, one can get the information on the depth (E_t) and frequency factor (ν_0) of the shallow traps. These parameters were obtained using the current × time *vs*. log time analysis (*cf.* Fig. 3b) [27] as $E_t = 0.57$ eV and $\nu_0 = 10^9$ s^{-1}. As it results from measurements with amorphous and crystalline samples [24], the traps may be characterized as "structural". Dark current-voltage characteristics of sandwich samples were typical of space-charge-limited currents (SCLC) [28]. In the low-voltage range, ($U < U_x = 4$ V; *cf.* curve 1 in Fig. 4), the current is proportional to the voltage. The superlinear region ($j \sim U^m$, $m = 1.6$) was found for higher voltages. The Ohmic current was proportional to the reciprocal sample thickness ($j \sim L^{-1}$), whereas the non-Ohmic current satisfied the relation $j \sim L^{-(2m-1)}$. The character of the current-voltage dependences under illumination was similar (curve 2 in Fig. 4). Ohmic photocurrent at low voltages was followed by a superlinear current-voltage dependence at higher voltages with $m = 1.7$.

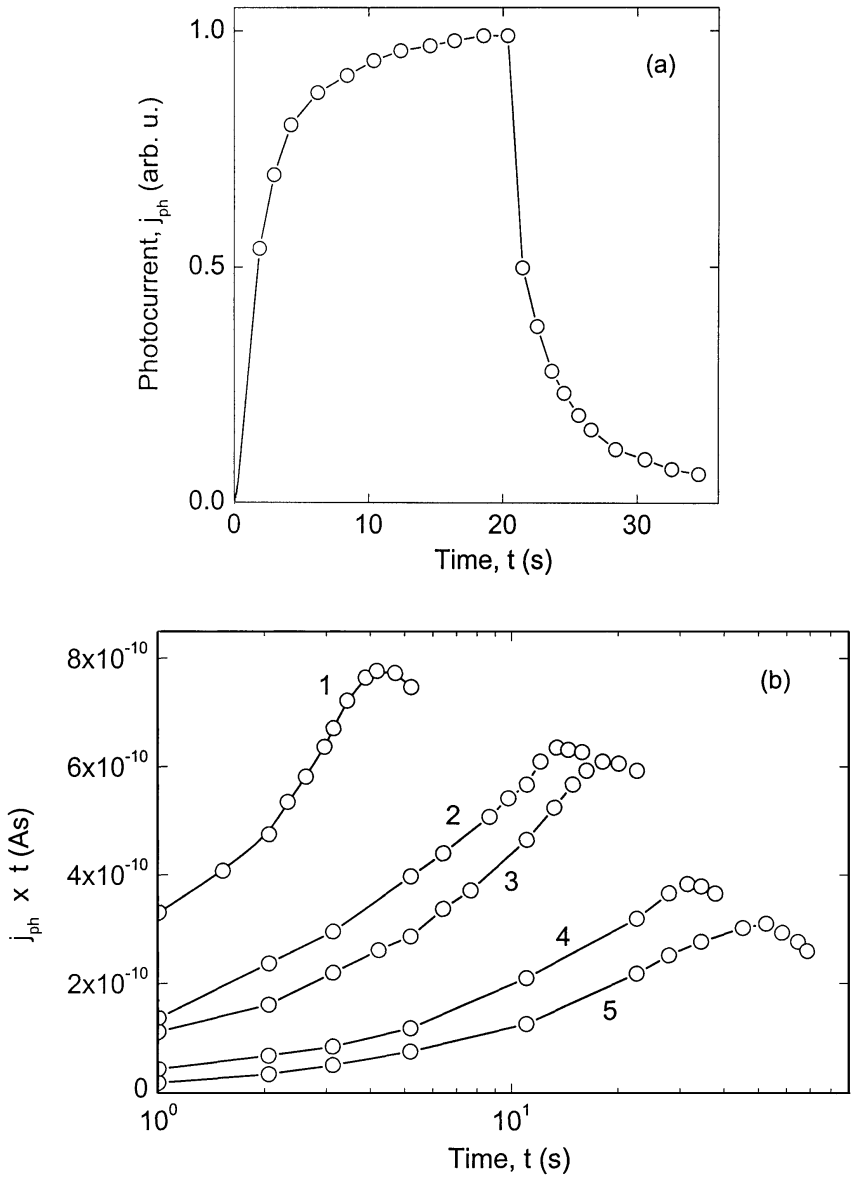

Figure 3. (a) Relaxation photocurrent process for DTA; λ = 625 nm, T = 219 K. (b) Isothermal decay curves measured at different temperatures. Curve 1 – T = 291 K, 2 – T = 282 K, 3 – T = 279 K, 4 – T = 267 K, 5 – T = 261 K.

Dielectric properties. Frequency dependences of the components of the complex electric permittivity ε*, *i.e.* ε′ and ε″, as well as of AC-conductivity σ_{AC}, are presented in Fig. 5. In the frequency range 1×10^1–3×10^4 Hz, the following dependences were obtained: $\varepsilon'' \sim f^{0.7}$ and $\sigma_{AC} \sim f^{0.3}$ (*cf.* curves 2 and 3 in Fig. 5). The real part of the complex electric permittivity was ε′ = 5.4 at 10 Hz. This value decreases with increas-

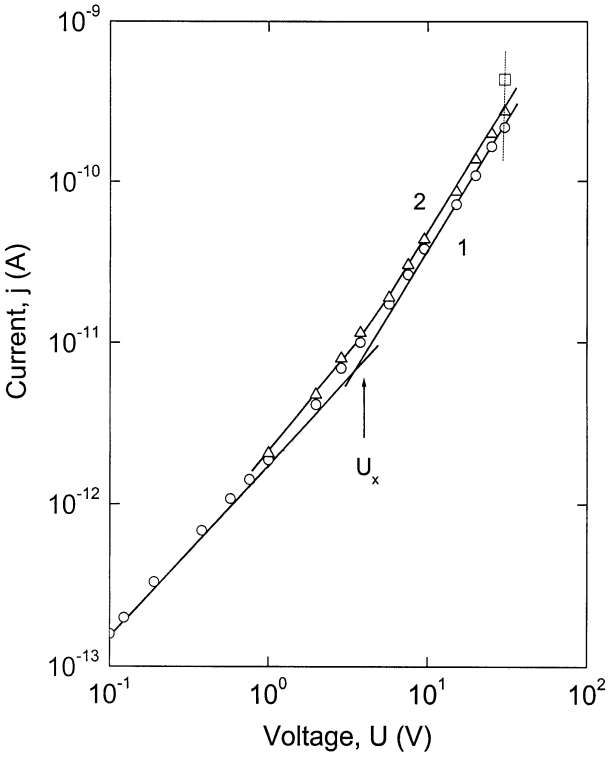

Figure 4. Steady-state current-voltage (*j-U*) characteristic of a DTA layer in the dark and under illumination. Curve 1 – in the dark, curve 2 – under 605 nm illumination. Photon flux $\phi = 2.6 \times 10^{12}$ photon cm^{-2} s^{-1}. ( ) photocurrent for $\phi = 3.8 \times 10^{13}$ photon cm^{-2} s^{-1}. Sample thickness $L = 10^{-2}$ cm.

ing frequency to 4.7 at 3×10^4 Hz. It is known that the dielectric relaxation process determines appropriate ε' and ε'' frequency dependences, which comprise the dispersion of this process [29]. The obtained ε^* *vs*. *f* dependence suggests that only a high-frequency part of dispersion is present.

The DTA layers exhibited a photodielectric effect. The change in the capacitance with illumination, ΔC, as a function of excitation wavelength, is given in Fig. 6a. The photodielectric response was found in the spectral region 400–750 nm. The well-developed maximum of the ΔC *vs*. λ dependence at 610 nm coincides with the photocurrent peak at 615 nm. The time dependence of ΔC made it possible to determine the photocapacitance relaxation time $\tau_{\Delta C}$. The results indicated that, besides the initial part ($t < 300$ s), where a more rapid photocapacitance increase took place, an exponential time dependence could be applied

$$\Delta C\,(t) = \Delta C_\infty\,[1 - \exp(-t/\tau_{\Delta C})] \qquad (1)$$

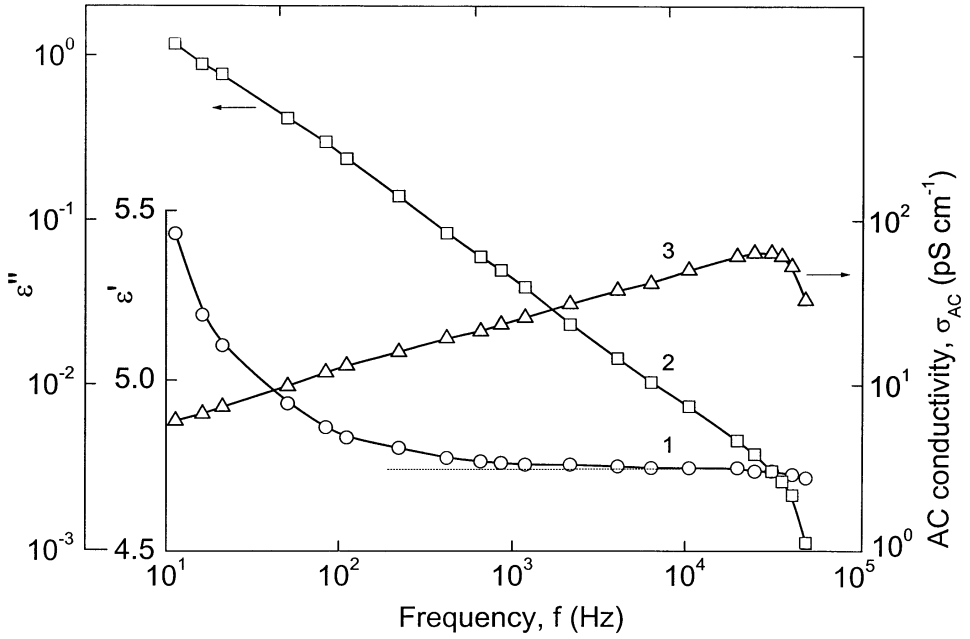

Figure 5. Frequency dependences of the complex electric permittivity components and AC dark conductivity. Curves 1, 2 and 3 – ε', ε'' and σ_{AC}, respectively. U_{AC} = 1 V.

where $\Delta C(t)$ is the photocapacitance at the time t and ΔC_∞ is the steady-state value of the photocapacitance. The wavelength dependence of $\tau_{\Delta C}$ is presented in Fig. 6b. The stepwise dependence clearly distinguishes two spectral regions. The mean values of $\tau_{\Delta C}$ were 1.5×10^3 s and 5×10^2 s for wavelengths shorter and longer than 580 nm, respectively. The photocapacitance is frequency- and light intensity-dependent. The ΔC *vs*. f dependence (curve 1 in Fig. 7) indicates that the photocapacitance decreases with frequency and this decrease is significantly pronounced at the high-frequency edge of the investigated frequency range. The frequency dependence of the dielectric loss ε''_λ under photoexcitation shows a similar tendency (*cf*. curve 2 in Fig. 7). Both ΔC and AC-photoconductivity $\Delta\sigma^{\lambda}_{AC}$ increase with a photon flux ϕ at given λ, possessing the same dependences, *i.e*. $\Delta C \sim \phi^q$, $\Delta\sigma^{\lambda}_{AC} \sim \phi^q$, as it follows from Fig. 8, with $q = 0.4$. Since, in the dark, the ratio of the DC-conductivity and AC-conductivity measured at 10 Hz (the lowest measurement frequency) is 3×10^{-3} and this ratio is of the same order of magnitude even under illumination, the losses in the dark ε'' and under illumination ε''_λ are assumed to be dielectric. It could be pointed out that both the photoelectric and (photo)dielectric characteristics obtained from the measurements were well reproducible. The scattering of the values obtained on different samples did not exceed 10%.

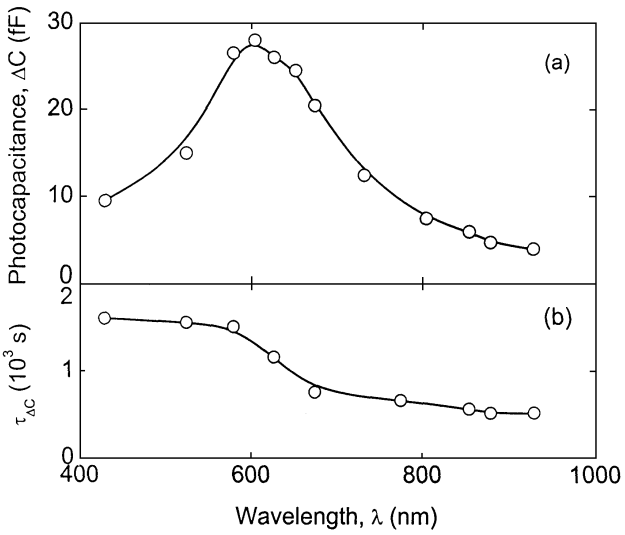

Figure 6. Action spectrum of the photocapacitance (a) and photodielectric relaxation time (b); $f = 10^3$ Hz, $\phi = 1.3 \times 10^{12}$ photon cm^{-2} s^{-1}.

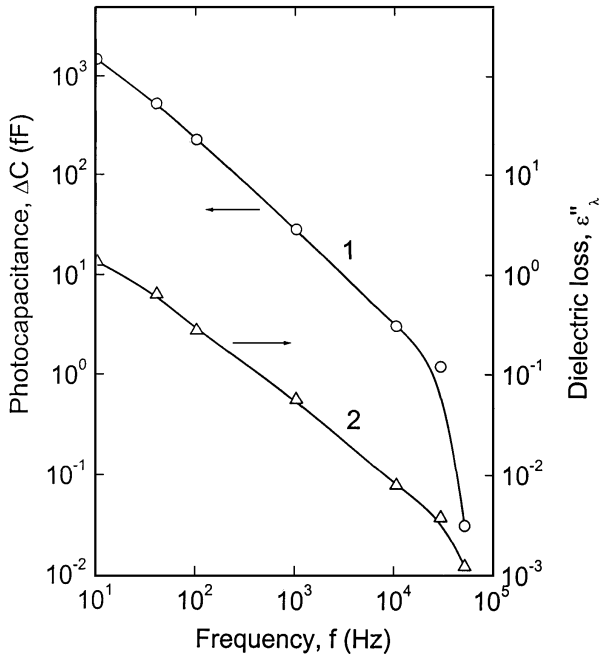

Figure 7. Frequency dependences of the photocapacitance (curve 1) and dielectric losses under photoexcitation ε''_λ (curve 2). $\lambda = 605$ nm, $\phi = 1.3 \times 10^{12}$ photon cm^{-2} s^{-1}.

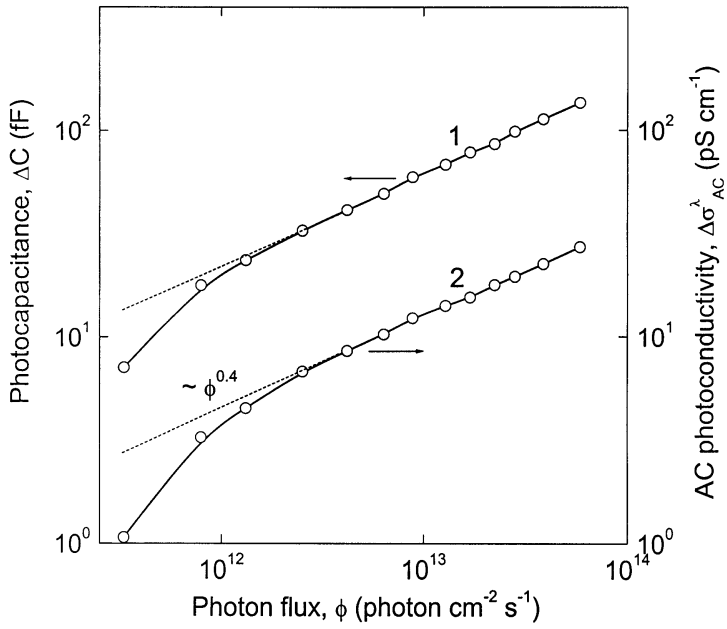

Figure 8. Dependence of the photocapacitance (curve 1) and AC photoconductivity increment (curve 2) on the photon flux; $\lambda = 655$ nm, $f = 10^3$ Hz.

Thin films of DTA are photoconductive. Their photoresponse followed roughly their absorption spectra when the contactless (xerographic) method was applied. The samples sandwiched between two SnO_2-covered glasses showed an additional peak at 615 nm, which could be attributed to the effect of surface states or of the space charge at the contact [30]. The influence of traps in the photoelectrical behaviour can also be suggested, judging from the shape of the current-voltage characteristics and from the dependences of the photocapacitance and photoconductivity on the photon flux (*cf.* Fig. 8). Rose [31] showed that in photoconductors containing traps, the q coefficient in the light intensity dependence of the photocurrent acquires values lower than 1 ($0.5 < q < 1$), depending on the ratio of the densities of free and trapped charge carriers. The value $q = 0.5$ was found in our experiments for polychromatic light. For monochromatic light, q was lower than 0.5, similarly to amorphous silicon. A possible explanation is the change in the mobility of charge carriers with their concentration in the layer, determined by the light penetration depth or by diffusion of the carriers from the region of their formation into the bulk and subsequent recombination in the bulk [32]. The photodielectric response was observed in the same spectral region as the steady-state photoconductivity. Thus, this effect seems to be associated with the free and trapped charge carriers, photogenerated in the sample bulk and in the precontact barrier interface layer. For $\lambda < 600$ nm, the photodielectric effect is very probably associated with the bulk properties, whereas for $\lambda > 600$ nm with a "preelectrode" interface layer, as it follows from a comparison of action spectra of the

photocapacitance, the photocurrent on the sandwich-contacted films, and the photoresponse obtained by contactless xerographic technique. The mean value of the photocapacitance relaxation time $\tau_{\Delta C}$ was 1.5×10^3 s for $\lambda < 600$ nm. Using the frequency factor 10^9 s^{-1}, as it was obtained from the photoconductivity isothermal decay curves, from $\tau_{\Delta C}$ the trap depth 0.7 eV results. This value is close to that obtained from the isothermal photocurrent kinetics, 0.6 eV, as well as to the activation energy of the photocurrent. The perceptible photocapacitance effect was observed for the frequencies $f < 3 \times 10^4$ Hz (at 293 K), showing a tendency to saturation of the dependence of ΔC on frequency at *ca*. 10 Hz (curve 1 in Fig. 7). This means, that photodielectric response is quite "slow" and cannot be directly associated with either the charge redistribution in the molecule during photoexcitation or the free photogenerated charge carrier formation; nevertheless, space charge and trapping phenomena play an important role. This finding is in agreement with a significantly large value of $\tau_{\Delta C}$, compared with the dielectric relaxation time obtained in the dark, τ_0, and under illumination, τ_0^{λ} and it is also supported by a sublinear dependence of the AC photoconductivity on the photon flux (*cf*. Fig. 8). The reason for this behavior could be the same as for the DC photoconductivity discussed above. The stepwise spectral $\tau_{\Delta C}$ dependence shows that, depending on wavelength, at least two different processes contribute to the photocapacitance effect. According to the Havriliak-Negami function approach [29], the investigation of dielectric relaxation phenomena gives the ε'' *vs*. ε' plot presented in Fig. 9. The data obtained in the dark and under illumination fit a sim-

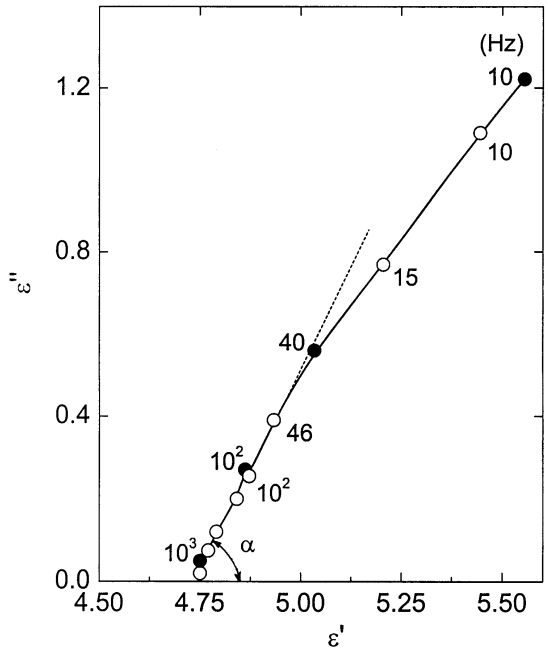

Figure 9. Plot of ε'' *vs*. ε' in the dark (open circles) and under illumination (full circles). $\lambda = 605$ nm, $\phi = 1.3 \times 10^{12}$ photon cm^{-2} s^{-1}.

ilar curve, the value of the limiting angle α being 1.1 rad in the high-frequency region (experimental points found under illumination are a little shifted to higher frequencies). It is well known that at high frequencies ($\omega\tau_0 >> 1$), the skewed circular arc equation

$$\varepsilon^* - \varepsilon = (\varepsilon_s' - \varepsilon') / [1 + (i\omega\tau_0)^{1-A}]^B \tag{2}$$

gives the limiting relations

$$\varepsilon'' = (\varepsilon_s' - \varepsilon') \sin[(1-A)B\,\pi/2]\,(\omega\tau_0)^{-(1-A)B} \tag{3}$$

and

$$B = 2\alpha/\pi(1-A) \tag{4}$$

where τ_0 is the mean dielectric relaxation time, ε_s' and ε' are values for zero and infinite frequencies ($\omega = 2\pi f$) of the proper dispersion region, respectively, A and B are empirical parameters, which determine the τ_0 distribution peculiarities [29,33]. In our case both relations (4) and (5) give $(1-A)B = 0.7$ (*cf.* curve 2 in Fig. 5 and Fig. 9). Taking into account the real values of A and B one obtains $0 < A \leq 0.3$ at $0.7 < B \leq 1$. This suggests that a dielectric relaxation time distribution occurs in DTA layers.

From the experimental data, obtained at low frequency (10 Hz), it was possible to determine $\tau_0 > 2 \times 10^{-2}$ s. The upper limit of τ_0 was estimated as follows. Using the experimental data from Fig. 5 (curve 2), (3) gives τ_0 equal to 5×10^{-2}, 1×10^{-1} and 3×10^{-1} s for $(\varepsilon_s' - \varepsilon')$ equal to 3, 5 and 10, respectively. Since for a proper dispersion region, $(\varepsilon_s' - \varepsilon')$ is of the order of ε''_{max} [34] and the highest measured ε'' value is 1.2 (Fig. 9), it seems quite reasonable that $\tau_0 < 3 \times 10^{-1}$ s. The shift in the ε'' *vs.* ε' plot between experimental points, obtained in the dark and under illumination indicates that $\tau_0^{\lambda} < \tau_0$, where τ_0^{λ} is the dielectric relaxation time under illumination. Generally, the photodielectric and photoconductivity phenomena in thin DTA layers are strongly influenced by the charge carrier formation under illumination. This suggests that the photodielectric effect in DTA layers can be explained by mechanism (iv), *i.e.* by a photoinduced increase in the free and trapped charge carrier concentration. The applicability of the conductivity hypothesis to our experimental results was tested by solving the system of differential equations bounding together the current density, electric field strength F and concentration of charge carriers in the sample of thickness L. The equations were published previously by Kneppo *et al.* [20] and Pillai *et al.* [35]. Assuming the steady-state case, immobile electrons (electron mobility $\mu_n = 0$) and open-circuit conditions (external circuit current $j = 0$), the fundamental system of differential equations reduces to

$$\frac{dF}{dx} = \frac{e}{\varepsilon'}\left[\Delta p + \Delta p_t - \frac{1}{\gamma(p_0 + \Delta p}(\eta\alpha\phi\exp(-Kx) - \gamma n_0 \Delta p)\right] \tag{5}$$

$$\frac{d\Delta p}{dx} = \frac{e}{kT}(p_0 + \Delta p)F \tag{6}$$

where e is the elementary charge, γ is the recombination coefficient, η photogeneration quantum efficiency, K absorption coefficient, ϕ photon flux, k Boltzmann constant, T temperature, $p_0(n_0)$ concentration of free holes (electrons) in thermal equilibrium, and Δp and Δp_t are changes in concentrations of free and trapped holes, respectively, under illumination. A single trap level approximation was used for the relation between free and trapped charge carriers in the form

$$\Delta p_t + p_{t0} = \frac{(p_0 + \Delta p)P_t}{p_1 + p_0 + \Delta p} \tag{7}$$

where P_t is the concentration of traps, $p_1 = N_v \exp(-E_t/kT)$, N_v being the effective concentration of states, E_t is the trap depth, and p_{t0} is the concentration of trapped holes in thermal equilibrium. To solve this system of equations, boundary conditions must be taken into account. Thus we assume that: (a) the sample is electrically neutral as a whole, from which follows $F(0) = F(L)$; (b) no external field is applied to the sample and, consequently, if no surface states are present, $F(0) = 0$. These boundary conditions differ from those published by Kneppo *et al*. [20] and Pillai *et al*. [35], who used the following ones: Δp and Δp_t are assumed to be zero at $x = \infty$, changes in electron and hole concentrations are equal for $x = 0$ (generally, this means that the sample under the steady-state conditions could not fulfil the neutrality condition for the one-carrier case). The authors [20,35] assumed small changes in charge carrier concentrations under illumination and, therefore, linearized (5) and (6). Their approach seems to be oversimplified. Generally, in the framework of the conductivity hypothesis, for the observable photodielectric effect, changes in charge carrier concentrations cannot be assumed to be low; hence, (5) and (6) cannot be linearized. Solving these equations under the above mentioned boundary conditions (a) and (b) the electrical conductivity $\sigma(x)$ can be calculated as

$$\sigma(x) = e\mu_p[p_0 + \Delta p(x)] \tag{8}$$

where μ_p is the hole mobility. The admittance Y of the sample can be then expressed as

$$Y = \frac{1}{R} + i\omega C = \left[\int_0^L \frac{dx}{\sigma(x) + i\omega\varepsilon} \right]^{-1} \tag{9}$$

where R is the sample resistance. The results of the model calculations are given in Figs. 10(a) and 10(b). The chosen parameters were: $L = 10^{-2}$ cm, relative electric permittivity $\varepsilon_r = 3$, $T = 300$ K, $N_v = 4 \times 10^{21}$ cm^{-3}, $P_t = 10^{14}$ cm^{-3}, $E_t = 0.6$ eV, $\gamma = 10^{-11}$ cm^3 s^{-1}, $p_0 = 10^6$ cm^{-3}, $p_{t0} = 3.03 \times 10^8$ cm^{-3}, $n_0 = 3.04 \times 10^8$ cm^{-3}, $K = 10^5$ cm^{-1}, $\eta = 10^{-6}$ charges per photon. Comparing the experimental (Figs. 6 and 7) and theoretical (Fig. 10) dependences, one can see, that theoretical values ΔC are higher than the experimental ones (*cf*. the values from Figs. 10(b) and 7): the theoretical value $\Delta C/C_0 = 10^{-1}$ for the photon flux of 10^{12} photon cm^{-2} s^{-1} (C_0 is the capacitance in the dark) is higher than the experimental value $\Delta C/C_0 = 10^{-3}$. The reason for this difference could be found in the charge carrier transport. In the theory we assumed delocalized transport in the band, whereas the frequency dependence σ_{AC} (curve 3 in Fig. 5) suggests the possibility of the adiabatic hopping transport [36]. Also trapping phenomena, which limit the charge carrier mobility, could play an important role.

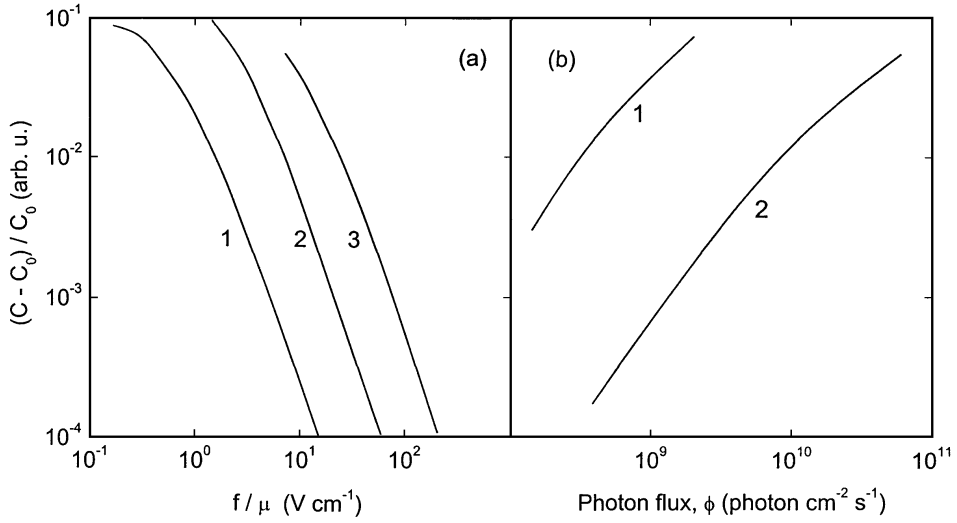

Figure 10. Theoretical dependences of relative photocapacitance $(C - C_0)/C_0$ on the ratio frequency/charge carrier mobility for different light intensities (a) (curve 1 – $\phi = 10^{10}$, curve 2 – $\phi = 10^{11}$, curve 3 – $\phi = 10^{12}$ photons cm^{-2} s^{-1}), and on light intensity for different ratios of frequency/charge carrier mobility (b) (curve 1 – $f/\mu = 1$, curve 2 – $f/\mu = 10$ V cm^{-2}).

Acknowledgments

The authors thank Dr. M. Tlust'áková for the synthesis of diethyl 2,5-dianilinoterephthalate and Mrs. D. Dundrová for technical assistance in preparation of the manuscript. The work was sponsored by the Grant Agency of the Academy of Sciences of the Czech Republic (grants No. A1050901 and AV0Z4050913).

REFERENCES

1. Karl N., Bauer A., Holzäpfel J., Marktanner J., Möbus M. and Stölzle F., *Mol. Cryst. Liq. Cryst.,* **252**, 243 (1994).
2. Kato K. and Braun C.L., *J. Chem. Phys.,* **72**, 172 (1980).
3. Signerski R., Kalinowski J., Koropecký I. and Nešpůrek S., *Thin Solid Films,* **121**, 175 (1984).
4. Silinsh E.A. and Jurgis A.J., *Chem. Phys.,* **94**, 77 (1985).
5. Valerián H. and Nešpůrek S., *J. Appl. Phys.,* **73**, 4370 (1993).
6. Shibahara S., Nishioka T., Natsume N., Ishikawa K., Takezoe H. and Fukuda A., *Synth. Met.*, **94**, 255 (1998).
7. Nešpůrek S. and Eckhardt A., *Polym. Adv. Technol.*, **12**, 427 (2001).
8. Hertel D., Bässler H., Möller S., Tillmann H. and Hörhold H.H., *Mol. Cryst. Liq. Cryst.*, **355**, 175 (2001).
9. Onsager L., *Phys. Rev.,* **54**, 554 (1938).
10. Liptay W., *Excited States,* ed. Lim E.C., Vol. 1, Academic Press, London, 1974.
11. Glazebrook R.W. and Thomas A., *J. Chem. Soc., Faraday Trans. 2,* **78**, 2053 (1982).
12. *Primary Photoexcitations in Conjugated Polymers: Molecular Exciton Versus Semiconductor Band Model*, ed. Sariciftci, World Scientific, Singapore, 1997.
13. Vardeng Z.V. and Wri X., *Synth. Met.*, **54**, 99 (1993).
14. Yu J.-W., Kim J.K., Cho H.N., Kim D.Y., Kim C.Y., Song N.W. and Kim D., *Macromol.*, **33**, 5443 (2000).
15. Krispin P. and Ludwig W., *Phys. Stat. Solidi,* **12**, 595 (1965).
16. Garlick G.F.J. and Gibson A.F., *Proc. Phys. Soc.,* **62 A**, 731 (1949).
17. Mark P. and Kallmann H., *J. Phys. Chem. Solids,* **23**, 1067 (1962).
18. Devi S. and Prkash S.G., *Ind. J. Pure Appl. Phys.*, **30**, 75 (1992).
19. Devi S. and Prkash S.G., *Natl. Acad. Sci. Lett.*, **14**, 453 (1991).
20. Kneppo I. and Cervenák J., *Solid-State Electronics,* **15**, 587 (1972).
21. Yang S.R. and Taylor K.N.R., *J. Appl. Phys.,* **67**, 3387 (1990).
22. Honzl J., Ulbert K., Hádek V., Tlust'áková M. and Metalová M., *J. Polym. Sci. C,* **16**, 4465 (1969).
23. Nešpůrek S., *Czech. J. Phys. B,* **23**, 368 (1973).
24. Nešpůrek S., Slavínská D. and Šorm M., *Czech. J. Phys. B,* **31**, 1144 (1981).
25. Liebermann H., *Lieb. Ann. Chem.,* **404**, 272 (1914).
26. Nešpůrek S. and Ulbert K., *Cs. Cas. Fyz. A,* **25**, 144 (1975).
27. Simmons J.G. and Tam M.C., *Phys. Rev. B,* **87**, 3706 (1973).
28. Nešpůrek S., *Czech. J. Phys. B,* **24**, 660 (1974).
29. Havriliak S. and Negami S., *Polymer,* **8**, 161 (1967).
30. Day P. and Price G.M., *J. Chem. Soc. A,* 236 (1969).
31. Rose A., *RCA Rev.,* **12**, 362 (1951).
32. Kearns D.R., Tollin G. and Calvin A., *J. Chem. Phys.,* **32**, 1020 (1960).
33. Schonhols A. and Schlosser E., *Prog. Coll. Polym. Sci.,* **78**, 24 (1988).
34. Mačkus P. and Poškus A., *Lithuanian Phys. J.,* **31**, 419 (1991).
35. Pillai P.K.C. and Nath R., *Phys. Status Solidi (a),* **37**, 491 (1976).
36. Pollak M. and Geballe T.H., *Phys. Rev.,* **122,** 1742 (1961).